Digalactosyldiacylglycerol Is Essential for Organization of the Membrane Structure in Etioplasts[1]

Sho Fujii,[a] Koichi Kobayashi,[a,b,2] Noriko Nagata,[c] Tatsuru Masuda,[d] and Hajime Wada[a]

[a]Department of Life Sciences, Graduate School of Arts and Sciences, University of Tokyo, Meguro-ku, Tokyo 153-8902, Japan
[b]Faculty of Liberal Arts and Sciences, Osaka Prefecture University, Sakai, Osaka 599-8531, Japan
[c]Department of Chemical and Biological Sciences, Faculty of Science, Japan Women's University, Bunkyo-ku, Tokyo 112-8681, Japan
[d]Department of General Systems Studies, Graduate School of Arts and Sciences, University of Tokyo, Meguro-ku, Tokyo 153-8902, Japan

ORCID IDs: 0000-0003-3726-4790 (K.K.); 0000-0002-0894-2049 (N.N.); 0000-0002-1585-5832 (T.M.)

Angiosperms germinated in the dark develop etioplasts, the chloroplast precursors, in cotyledon cells. Etioplasts contain lattice membrane structures called prolamellar bodies (PLBs) and lamellar prothylakoids as internal membrane systems. PLBs accumulate the chlorophyll intermediate protochlorophyllide (Pchlide) in a complex with NADPH and light-dependent NADPH:Pchlide oxidoreductase (LPOR). Two galactolipids, monogalactosyldiacylglycerol and digalactosyldiacylglycerol (DGDG), are major constituents of etioplast membranes. We previously reported that monogalactosyldiacylglycerol facilitates the synthesis of Pchlide and the formation of the Pchlide-LPOR-NADPH complex in etioplasts, but the importance of DGDG in etioplasts is still unknown. To determine the role of DGDG in etioplast development and functions, we characterized a knockout mutant (*dgd1*) of Arabidopsis (*Arabidopsis thaliana*) *DGD1*, which encodes the major isoform of DGDG synthase, in the etioplast development stage. In etiolated *dgd1* seedlings, DGDG content decreased to 20% of the wild-type level, the lattice structure of PLBs was disordered, and the development of prothylakoids was impaired. In addition, membrane-associated processes of Pchlide biosynthesis, formation of the Pchlide-LPOR-NADPH complex, and dissociation of the complex after the photoconversion of Pchlide to chlorophyllide were impaired in *dgd1*, although the photoconversion reaction by LPOR was not affected by the DGDG deficiency. Total carotenoid content also decreased in etiolated *dgd1* seedlings, but the carotenoid composition was unchanged. Our data demonstrate a deep involvement of DGDG in the formation of the internal membrane structures in etioplasts as well as in membrane-associated processes of pigment biosynthesis and pigment-protein complex organization.

Prolamellar bodies (PLBs) are unique lattice membrane structures observed in etioplasts developed in cotyledon cells of dark-germinated angiosperms (Solymosi and Schoefs, 2010). In etioplasts, instead of chlorophyll (Chl), a Chl intermediate, protochlorophyllide (Pchlide), accumulates and forms a ternary complex with NADPH and light-dependent NADPH:Pchlide oxidoreductase (LPOR; Schoefs and Franck, 2003; Masuda, 2008). Most of the ternary complex is oligomerized and bound to the PLB membrane (Schoefs and Franck, 2003). In the ternary complex, light absorbed by the so-called photoactive Pchlide immediately activates LPOR to reduce Pchlide in the complex to chlorophyllide (Chlide), the last precursor of Chl, by using NADPH (Heyes and Hunter, 2005). By contrast, a portion of Pchlide, which is unbound to the active site of LPOR, is not immediately converted to Chlide after light exposure, so it is referred to as nonphotoactive Pchlide.

After photoconversion, the Chlide-LPOR-$NADP^+$ oligomeric complex is processed in a complicated manner (Schoefs et al., 2000; Schoefs, 2001). In the majority of the Chlide-LPOR-$NADP^+$ complex, $NADP^+$ is replaced by NADPH, followed by dissociation of the oligomeric complex to a dimeric Chlide-LPOR-NADPH complex. Subsequently, Chlide in this complex is replaced by Pchlide to regenerate the photoactive Pchlide-LPOR-NAPDH complex. In addition, a small portion of the oligomeric Chlide-LPOR-$NADP^+$ complex exchanges Chlide for Pchlide prior to replacing the cofactor to rapidly regenerate the oligomeric Pchlide-LPOR-NADPH complex (Franck et al., 1999). Finally, Chl synthase esterifies Chlide with a geranylgeranyl diphosphate, followed by three successive hydrogenation reactions of the geranylgeraniol moiety to yield Chl (Oster and Rüdiger, 1997; Schoefs and Bertrand, 2000).

[1]This work was supported by the Japan Society for the Promotion of Science (KAKENHI no. 16J10176 to S.F., no. 26711016 to K.K., and no. 26440170 to N.N.).

[2]Address correspondence to kkobayashi@las.osakafu-u.ac.jp.

The author responsible for distribution of materials integral to the findings presented in this article in accordance with the policy described in the Instructions for Authors (www.plantphysiol.org) is: Koichi Kobayashi (kkobayashi@las.osakafu-u.ac.jp).

S.F. designed and performed most experiments, analyzed the data, and wrote the article; K.K. conceived the project, designed the study, and wrote the article; N.N. performed electron microscopic analysis; T.M. and H.W. supervised and complemented the writing.

www.plantphysiol.org/cgi/doi/10.1104/pp.18.00227

In plants, tetrapyrroles, including Pchlide, are synthesized in plastids. The first important step of tetrapyrrole biosynthesis is the formation of 5-aminolevulinic acid (ALA) from the starting material glutamyl-tRNA^{Glu}, the rate-limiting step of the pathway (Beale, 1999; Brzezowski et al., 2015). Subsequently, ALA is transformed to protoporphyrin IX (Proto IX), the last common precursor of heme and Chl, via several enzymatic steps (Tanaka et al., 2011). For the Chl biosynthesis pathway, Proto IX is converted sequentially to Mg-Proto IX by Mg-chelatase (MgCh), Mg-Proto IX monomethylester (Mg-Proto IX ME) by *S*-adenosyl-L-Met:Mg-Proto IX methyltransferase (MgMT), and Pchlide by Mg-Proto IX ME cyclase (MgCY; Tanaka et al., 2011).

The 3D lattice structure of PLBs is composed of tubules formed from lipid bilayer membranes (Williams et al., 1998) with a high lipid-to-protein ratio (Selstam and Sandelius, 1984). Similar to the thylakoid membrane in chloroplasts (Dorne et al., 1990), in PLBs of wheat (*Triticum aestivum*) etioplasts, two galactolipids, namely, monogalactosyldiacylglycerol (MGDG) and digalactosyldiacylglycerol (DGDG), account for ~50% and ~30%, respectively, of the total membrane lipids (Selstam and Sandelius, 1984). In etioplasts, lamellar prothylakoid (PT) membranes are expanded from PLBs (Solymosi and Schoefs, 2010). The ratio of MGDG to DGDG is lower in PTs than in PLBs; MGDG and DGDG constitute 45% and 40%, respectively, of membrane lipids in wheat PTs (Selstam and Sandelius, 1984).

Arabidopsis (*Arabidopsis thaliana*) has three paralogs of MGDG synthase (MGD1, MGD2, and MGD3), which transfer the Gal in UDP-Gal to diacylglycerol to synthesize MGDG (Benning and Ohta, 2005). Inner envelope-localized MGD1 synthesizes most of the MGDG in chloroplasts, whereas outer envelope-localized MGD2 and MGD3 provide MGDG as a substrate for DGDG biosynthesis, especially under phosphate-deficient conditions (Kobayashi et al., 2009b). For DGDG biosynthesis, two paralogs of DGDG synthase, DGD1 and DGD2, catalyze the galactosylation of MGDG with a UDP-Gal (Benning and Ohta, 2005). Both isoforms are targeted to the outer envelope of chloroplasts; DGD1 is responsible for most of the DGDG biosynthesis and DGD2 works mainly under phosphate-deficient conditions with MGD2 and MGD3 (Kobayashi et al., 2009b). Knockout mutations of DGD1 (*dgd1*) but not DGD2 (*dgd2*) strongly decreased DGDG content without largely changing MGDG content (Dörmann et al., 1995; Kelly et al., 2003). A double knockout mutant of DGD1 and DGD2 (*dgd1 dgd2*) had almost no DGDG content and slightly reduced MGDG content (Kelly et al., 2003). The trace amount of DGDG in the *dgd1 dgd2* double mutant may be attributed to the activity of SENSITIVE TO FREEZING2 (SFR2), which transfers a Gal residue from MGDG to a second galactolipid to yield oligogalactolipids, including DGDG (Moellering et al., 2010). SFR2 is activated by freezing and contributes only marginally to galactolipid metabolism under nonfreezing conditions (Moellering et al., 2010).

As in chloroplasts, in etioplasts, MGD1 is mainly responsible for MGDG biosynthesis (Fujii et al., 2017), and the contributions of MGD2 and MGD3 are negligible (Kobayashi et al., 2009a). A 70% reduction in the mRNA level of *MGD1* by an artificial microRNA targeting *MGD1* (*amiR-MGD1*) decreased the MGDG content by 36% without affecting DGDG content in etiolated seedlings. The 36% loss of MGDG in *amiR-MGD1* only slightly changed the crystalline structure of PLBs but strongly inhibited Pchlide biosynthesis and the formation of the Pchlide-LPOR-NADPH ternary complex and its oligomerization (Fujii et al., 2017). Together with in vitro data showing that MGDG is required for oligomerization of the ternary complex (Gabruk et al., 2017), these results suggest that MGDG is an essential lipid component for Pchlide biosynthesis and the formation of Pchlide-LPOR complexes.

However, the roles of DGDG in etioplast biogenesis and functions remain unknown. To determine how DGDG is involved in etioplast development, we analyzed the membrane structures of etioplasts, the biosynthesis and accumulation of Pchlide, and the functions of the Pchlide-LPOR-NADPH complex in etiolated Arabidopsis *dgd1* seedlings.

RESULTS

DGD1 Synthesizes the Bulk of DGDG in Etioplasts

To determine the role of DGD1 in etioplast biogenesis, we analyzed galactolipid content in 4-d-old etiolated wild-type and *dgd1* seedlings. In *dgd1*, the proportions of MGDG and DGDG in total membrane lipids were decreased to 84% and 20% of wild-type levels, respectively (Fig. 1A). We further confirmed that the absolute amount of DGDG was drastically lower in *dgd1* seedlings, whereas that of MGDG and the total content of other membrane glycerolipids were not changed significantly (Supplemental Fig. S1). We also compared the fatty acid composition of galactolipids between the wild-type and *dgd1* seedlings. The proportion of 16:3 fatty acids in MGDG was decreased and that of 18:3 fatty acids was increased in *dgd1* seedlings (Fig. 1B). By contrast, the proportion of 18:3 fatty acids in DGDG was decreased greatly and that of other fatty acids was increased in *dgd1* seedlings (Fig. 1C).

DGDG Deficiency Perturbs the Membrane Structure in Etioplasts

To assess the contribution of DGDG to membrane formation in etioplasts, we observed the ultrastructure of etioplasts in wild-type and *dgd1* cotyledons (Fig. 2; Supplemental Fig. S2). Etioplasts of the wild-type cotyledons developed PLBs with a highly regular lattice structure and long PTs connected to PLBs (Fig. 2, A and B; Supplemental Fig. S2, A–D). In *dgd1* etioplasts, the

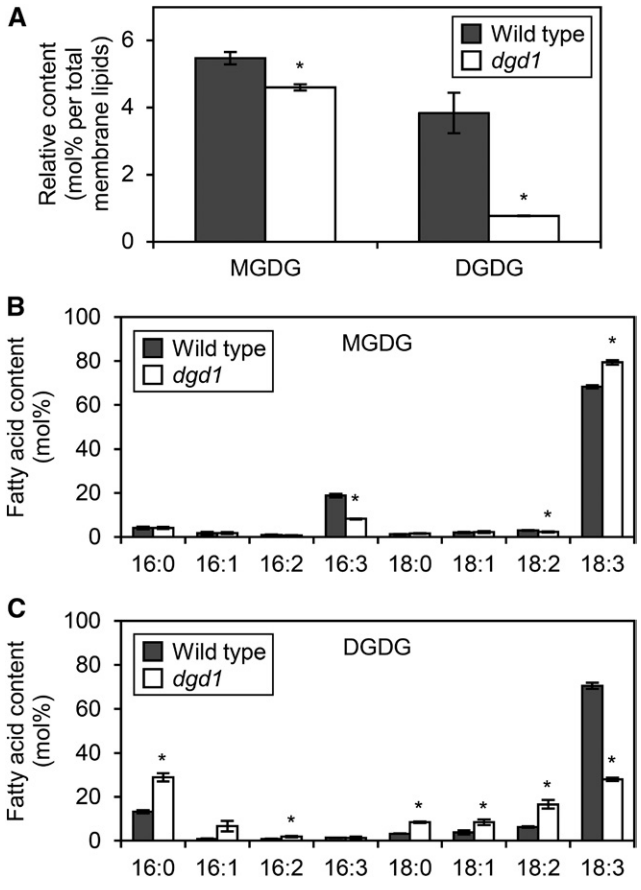

Figure 1. Galactolipid biosynthesis in 4-d-old etiolated wild-type and *dgd1* seedlings. A, Relative content of galactolipids in total membrane lipids. B and C, Fatty acid composition of MGDG (B) and DGDG (C). Data are presented as means ± SE from three independent experiments. Asterisks indicate significant differences from the wild type (*, $P < 0.05$, Student's *t* test).

lattice structure of PLBs was remarkably disordered and the development of PTs was strongly impaired (Fig. 2, C and D; Supplemental Fig. S2, E–H). We quantified the morphological changes in *dgd1* etioplasts. The relative SD value of the PLB unit size, an index of the irregularity of the PLB lattice (Fujii et al., 2017), was higher in *dgd1* than in the wild type (Fig. 2E), although the average size of the single PLB unit was not significantly different (Fig. 2F). We observed the presence of two or more PLBs in a single etioplast cross section, a state defined as fragmentation of PLBs, more frequently in *dgd1* (16 of 48 total etioplasts) than in the wild type (three of 38; Fig. 2, C and G; Supplemental Fig. S2H). In addition, the proportion of misshapen PLBs with low circularity was higher in *dgd1* cotyledons than in the wild type (Fig. 2G), but the overall size of PLBs was comparable in both genotypes (Fig. 2H). Moreover, the etioplasts in *dgd1* cotyledons had no PTs or markedly shorter ones than those in the wild type (Fig. 2I). Etioplasts had a rounder outline (Fig. 2J) and were larger (Fig. 2K) in *dgd1* cotyledons than in the wild type.

DGDG Deficiency Impairs the Accumulation of Pchlide and LPOR

To investigate the role of DGDG in Pchlide accumulation, we quantified Pchlide content in 4-d-old etiolated seedlings (Fig. 3A). In *dgd1*, total Pchlide content per seedling decreased to 76% of the wild-type level, although the size of etiolated cotyledons (Fig. 3B) and the fresh and dry weights of etiolated seedlings (Supplemental Fig. S3) were not changed. Etioplasts accumulate Pchlide in two states: a photoactive form that is photoreduced to Chlide immediately upon irradiation with a short flash of light, and a nonphotoactive form that is not photoreduced by a short flash treatment (Schoefs, 2001). The amount of Pchlide remaining after a 0.7-ms flash treatment, which corresponded to that of nonphotoactive Pchlide, was not significantly lower in *dgd1* than in the wild type (Fig. 3A). Thus, the decrease in total Pchlide content by the *dgd1* mutation was due mainly to a decrease in the photoactive form. Because photoactive Pchlide content is related to LPOR levels (Sperling et al., 1998; Franck et al., 2000; Masuda et al., 2003), we determined LPOR levels in the etiolated wild-type and *dgd1* seedlings by using polyclonal anti-LPOR antibodies that react with all three isoforms of Arabidopsis LPORs (PORA, PORB, and PORC; Rowe and Griffiths, 1995; Masuda et al., 2003; Fig. 3C). In *dgd1*, the total LPOR levels decreased to ~50% of the wild-type level. To explore the mechanism underlying the decrease in LPOR protein level, we evaluated steady-state mRNA levels of *PORA*, *PORB*, and *PORC* by reverse transcription quantitative PCR (Fig. 3D). The mRNA levels of *PORA* and *PORB*, the major isoforms in etiolated seedlings with high expression levels in the dark (Oosawa et al., 2000; Su et al., 2001), were similar in *dgd1* and wild-type seedlings. *PORC* is a minor isoform whose expression is much lower than that of *PORA* and *PORB* in the dark (Oosawa et al., 2000; Su et al., 2001). The mean expression of *PORC* was lower, but not significantly, in *dgd1* than in the wild type.

Pchlide Intermediates Accumulate in Excessive Amounts in *dgd1* with ALA Feeding

To examine the effect of DGDG deficiency on the Pchlide biosynthesis pathway, we measured the accumulation of porphyrin pigments in etiolated wild-type and *dgd1* seedlings treated with ALA for 1.5 h (Fig. 3E) and 24 h (Fig. 3F) in the dark. In the wild-type seedlings, ALA feeding induced a large accumulation of Pchlide, with only a slight accumulation of its intermediates. In the *dgd1* mutant, Pchlide accumulation was inhibited to 65% of the wild-type level after 1.5 h of ALA feeding, and instead, Mg-Proto IX accumulated in large amounts, with a slight increase in Proto IX content. After 24 h of ALA feeding, in addition to Proto IX and Mg-Proto IX, Mg-Proto IX ME accumulated in the mutant and Pchlide production decreased.

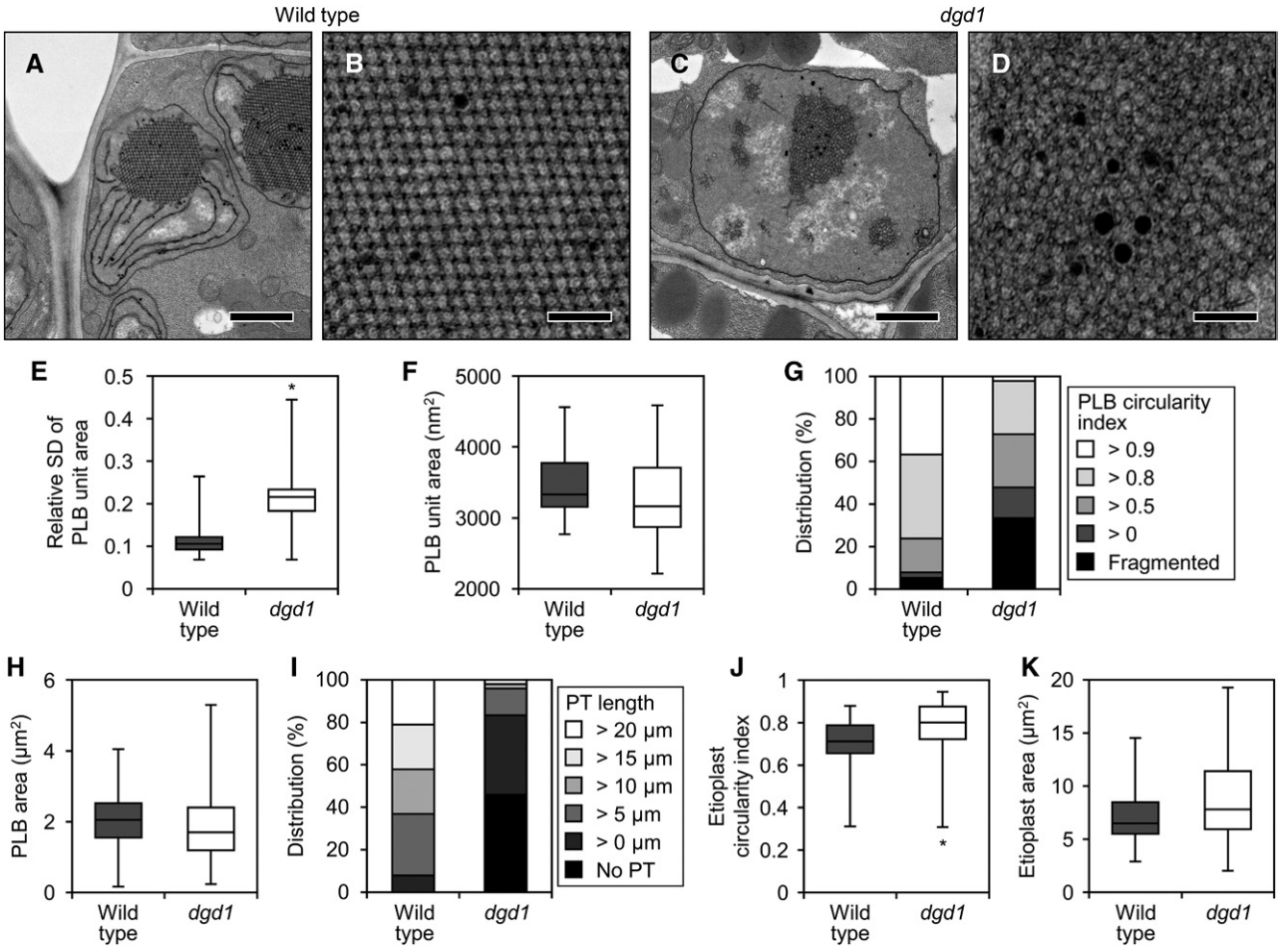

Figure 2. Ultrastructure of etioplasts in 4-d-old etiolated wild-type and *dgd1* seedlings. A and C, Images of whole etioplasts in etiolated cotyledons of the wild type (A) and *dgd1* (C). Bars = 1 μm. B and D, Magnified images of the PLBs in A (B) and C (D). Bars = 200 nm. E, F, H, J, and K, Quantitative data of relative SD value (SD/average) of the unit area in a PLB (E), area of a single PLB unit (F), area of PLBs (H), and circularity index (J) and area (K) of etioplasts. The horizontal line in each box represents the median value of the distribution. The top and bottom of each box represent the upper and lower quartiles, respectively. The whiskers represent the range. Data were obtained from 38 (wild type) and 48 (*dgd1*) different etioplasts. In E, the relative SD value was calculated from 20 units of the PLB in each etioplast. Asterisks indicate significant differences from the wild type (*, $P < 0.05$, Welch's *t* test). G and I, Distribution of the circularity index of PLBs (G) and length of PTs (I). Etioplasts with two or more PLBs were sorted as Fragmented in G, and those with no PTs were sorted as No PT in I. Data were obtained from 38 (wild type) and 48 (*dgd1*) different etioplasts.

DGDG Deficiency Perturbs the Fluorescence Shift after Photoconversion of Pchlide to Chlide

To determine the role of DGDG in the organization of the Pchlide-LPOR-NADPH complex, we measured fluorescence spectra at 77K in etiolated cotyledons of the wild type and *dgd1* (Fig. 4A). Under 77K, nonphotoactive and photoactive Pchlide can be distinguished by their unique fluorescence bands at ~633 and ~655 nm, respectively (Schoefs, 2001). Under our experimental conditions, wild-type seedlings emitted two fluorescence bands peaking at 630 and 653 nm, which were attributed to nonphotoactive and photoactive Pchlide, respectively (Fujii et al., 2017). After a 0.7-ms flash treatment, only the 653-nm peak disappeared, and instead, a new emission band, attributed to oligomeric Chlide-LPOR-NADP$^+$ complexes (Schoefs, 2001), emerged at ~689 nm (Fig. 4B). Similar emission spectra were observed for *dgd1* seedlings before and after the flash treatment.

After photoconversion, the fluorescence band at ~689 nm gradually shifted to ~680 nm in the dark, presumably reflecting the dissociation of the oligomeric Chlide-LPOR-NADP$^+$ complex to the dimeric complex (Shibata, 1957; Schoefs, 2001; Smeller et al., 2003; Solymosi et al., 2007). In wild-type seedlings, the peak at 689 nm shifted to 687 nm after 5 min of dark incubation, with a shoulder appearing at ~680 nm (Fig. 4C). After 10 min, a sharp band was observed at 679 nm (Fig. 4D) and shifted further to 678 nm after 20 min

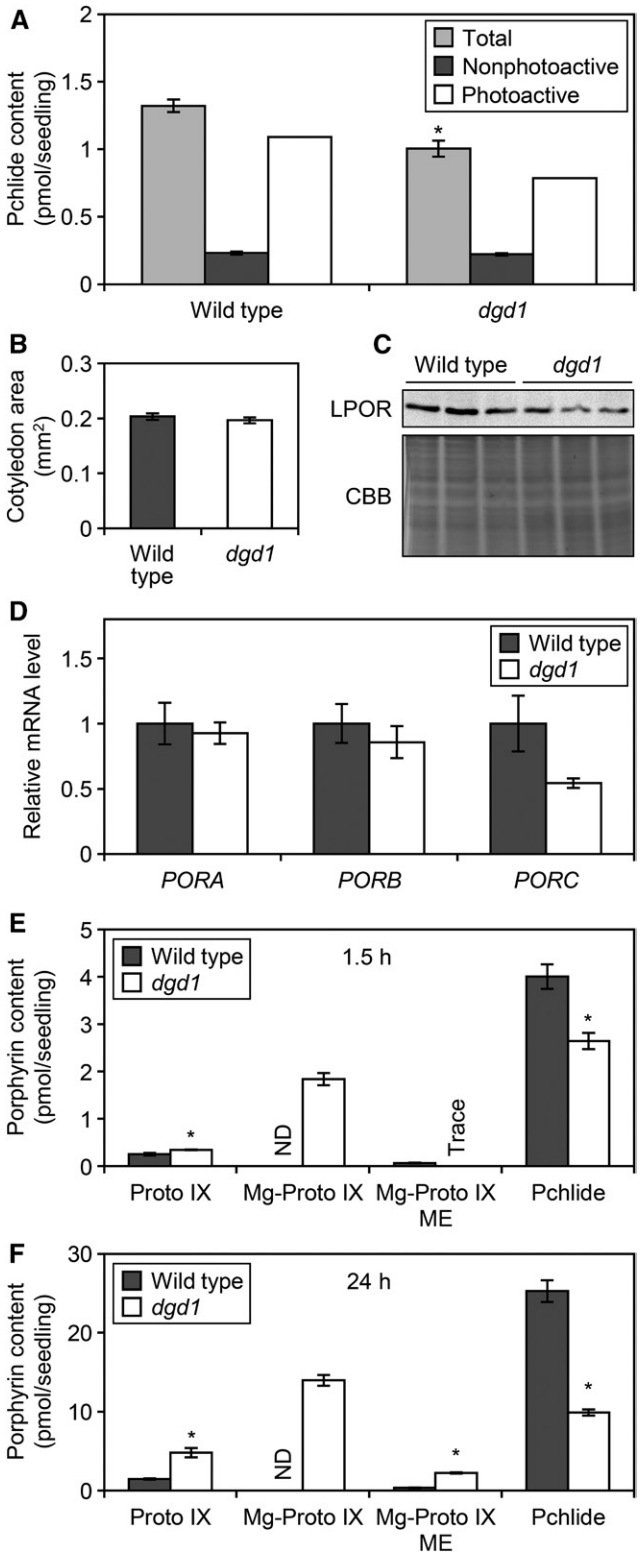

Figure 3. Altered Pchlide metabolism in *dgd1*. A, Pchlide content in 4-d-old etiolated wild-type and *dgd1* seedlings. Total and nonphotoactive Pchlides were extracted before and after flash treatment, respectively. Data are represented as means ± SE from 12 independent experiments. The amount of photoactive Pchlide was estimated by subtracting the amount of nonphotoactive Pchlide from total Pchlide. B, Size of 4-d-old etiolated cotyledons. Data are represented as means ± SE from 60 seedlings. C, Immunoblot analysis of total LPOR protein levels (~37 kD) in 4-d-old etiolated seedlings. Results of three biologically independent samples are shown. CBB denotes Coomassie Brilliant Blue-stained proteins between 25 and 50 kD, which served as loading controls. D, Reverse transcription quantitative PCR analysis of LPOR genes in 4-d-old etiolated seedlings. Data are represented as means ± SE from six independent experiments. E and F, Accumulation of porphyrin pigments in 4-d-old etiolated seedlings treated with ALA for 1.5 h (E) and 24 h (F) in the dark. ND, Not detected. Data are represented as means ± SE from three independent experiments. Asterisks indicate significant differences from the wild type (*, $P < 0.05$, Student's *t* test).

(Fig. 4E). The peak at ~678 nm remained until 2 h after the flash treatment (Fig. 4F). The stepwise shift of peak wavelengths of Chlide fluorescence is quantified in Figure 4G. This process, the so-called Shibata shift, progressed more slowly in *dgd1* than in the wild type. In the mutant, the fluorescence peak from Chlide was slightly red shifted after 5 min of incubation and then blue shifted to 682 and 681 nm after 10 and 20 min, respectively (Fig. 4, C–E). After 2 h, the Chlide fluorescence band was observed at 678 nm in *dgd1* as in the wild type (Fig. 4F).

In addition to the delayed Shibata shift, regeneration of the fluorescence band at 655 nm from photoactive Pchlide was retarded in *dgd1* seedlings. In *dgd1*, a 655-nm peak was not observed until 20 min after photoconversion, whereas that in the wild type appeared already after 5 min of incubation (Fig. 4, C–E).

DGDG Deficiency Decreases Carotenoid Accumulation But Does Not Notably Affect Its Composition

Carotenoids also are involved in the formation of the PLB structure (Solymosi and Schoefs, 2010). To determine the effect of DGDG deficiency on carotenoid accumulation in etiolated seedlings, we measured total carotenoid content in *dgd1* seedlings (Fig. 5A). Total carotenoid content in *dgd1* decreased to 66% of the wild-type level, which suggested that DGDG deficiency affected carotenoid metabolism in etiolated seedlings. To investigate which steps of carotenoid metabolism were affected by the *dgd1* mutation, we quantified the content of each carotenoid by HPLC at an absorbance of 447 nm (Fig. 5B). Consistent with the findings reported previously for a membrane extract from etiolated wheat seedlings (Ouazzani Chahdi et al., 1998), our results showed six types of carotenoids, namely, neoxanthin, violaxanthin, antheraxanthin, lutein, zeaxanthin, and β-carotene, in etiolated wild-type and *dgd1* seedlings. In *dgd1*, the contents of most carotenoid species decreased, but their composition did not differ greatly from that in the wild type (Fig. 5, B and C). A small increase in the proportion of antheraxanthin and zeaxanthin in *dgd1* might be attributed to an enhanced conversion of violaxanthin to antheraxanthin and zeaxanthin in response to the increased MGDG-to-DGDG ratio, because violaxanthin deepoxidase, which catalyzes these steps, is known to be

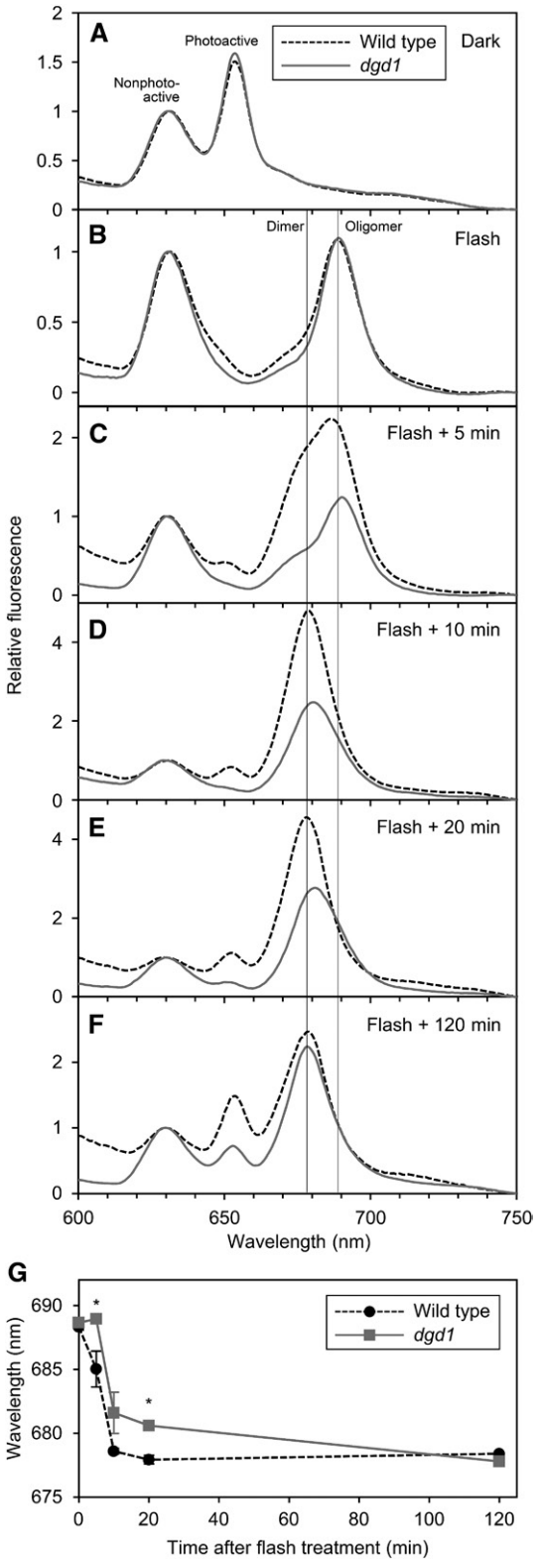

Figure 4. In situ 77K fluorescence spectra in 4-d-old etiolated cotyledons of the wild type and *dgd1* under 440-nm excitation. A and B, Fluorescence spectra in cotyledons frozen before (A) and immediately after (B) the flash treatment. C to F, Fluorescence spectra in cotyledons frozen after dark incubation for 5 min (C), 10 min (D), 20 min (E), and 120 min (F) after the flash treatment. Representative data from three (wild type at 0, 10, 20, and 120 min and *dgd1* at 0, 10, and 120 min), four (*dgd1* at 20 min), five (*dgd1* at 5 min), and six (wild type at 5 min) biologically independent experiments are shown. In B to F, vertical lines indicate the peak wavelength of oligomeric Chlide-LPOR-$NADP^+$ complex (Oligomer) and dimeric Chlide-LPOR-NADPH complex (Dimer). G, Overview of the Shibata shift after the flash treatment. Data are represented as means ± SE from three to six independent experiments. Asterisks indicate significant differences from the wild type (*, $P < 0.05$, Student's *t* test).

activated in an MGDG-rich environment (Schaller et al., 2010). Notably, carotenoid intermediates, such as ζ-carotene, proneurosporene, and prolycopene, whose overaccumulation perturbs the structure of the PLB lattice (Park et al., 2002), were not detected in *dgd1* or in the wild type in our HPLC analysis.

DISCUSSION

DGD1 Is the Major DGDG Synthase in Etioplasts

An 80% decrease in DGDG content in etiolated *dgd1* seedlings indicates that DGD1 is the main enzyme for DGDG synthesis in etioplasts (Fig. 1A). The remaining DGDG in *dgd1* can be synthesized by DGD2 and/or SFR2. Considering that SFR2 plays a specific role in freezing responses and is inactive under standard growth conditions (Moellering et al., 2010), DGD2 is thought to contribute mainly to DGDG biosynthesis in etiolated *dgd1* seedlings as in light-grown *dgd1* plants (Kelly et al., 2003). This assumption is supported by the finding that DGDG in the etiolated *dgd1* seedlings contained more palmitic acid (16:0) and less linolenic acid (18:3), a feature of DGDG molecules synthesized by DGD2 (Kelly et al., 2003). Together with the evidence that MGD1 is the primary MGDG synthase in etioplasts (Fujii et al., 2017), our findings indicate that MGD1 and DGD1 play the central role in galactolipid biosynthesis in etioplasts as well as in chloroplasts.

DGDG Is Required for the Formation of the Regular Lattice Structure of PLBs and Elongation of PTs

The 80% loss of DGDG in *dgd1*, which increased the MGDG-to-DGDG ratio to 6, strongly disrupted the round shape and lattice structure of PLBs (Fig. 2, A–E and G). We recently showed that a 36% loss of MGDG, resulting in almost equivalent MGDG and DGDG amounts in etiolated seedlings, slightly disrupted the shape and lattice structure of PLBs. Consistent with this finding was that of an in vitro experiment, which showed that both non-bilayer-forming MGDG and bilayer-forming DGDG are necessary for the formation of the PLB-like cubic structure in the mixture of lipids and water (Brentel et al., 1985). Thus, an MGDG-to-DGDG ratio of approximately 1.5 in the wild type may be important for maintaining regular PLB structures, as proposed previously (Selstam and Sandelius, 1984). In

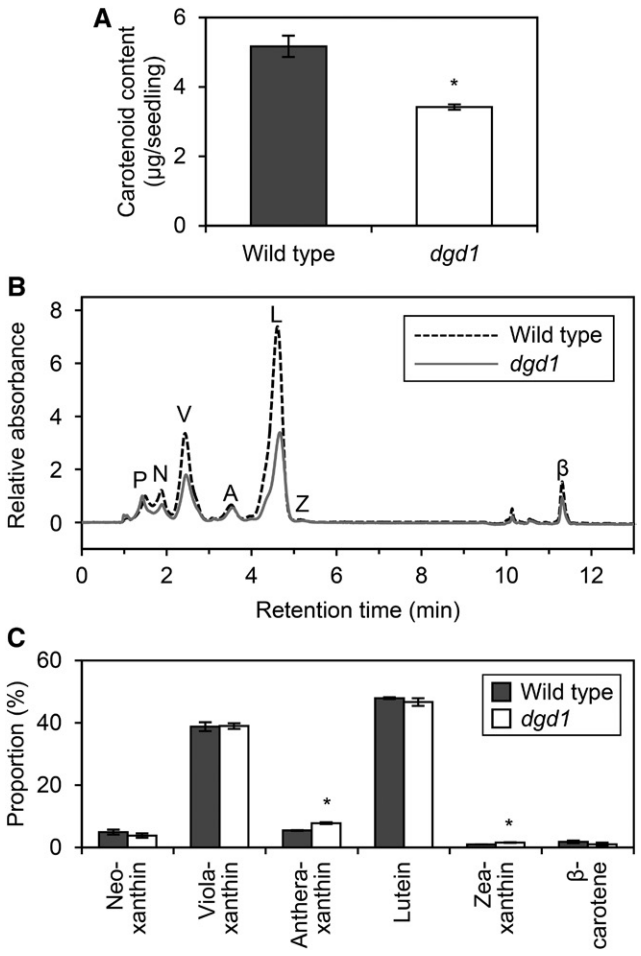

Figure 5. Carotenoid accumulation in 4-d-old etiolated wild-type and *dgd1* seedlings. A, Total carotenoid content. Data are represented as means ± SE from six independent experiments. B, HPLC trace of extracted pigments from etiolated seedlings. Absorbance at 447 nm was monitored. Representative data from three independent experiments are shown. The trace was normalized at the peak of Pchlide as 1 and the absorbance at 0 min as 0. The letters P, N, V, A, L, Z, and β indicate peaks of Pchlide, neoxanthin, violaxanthin, antheraxanthin, lutein, zeaxanthin, and β-carotene, respectively. We also detected a small peak of chlorophyll *a* at ~10 min. C, Proportion of carotenoid pigments. Data are means ± SE from three independent experiments. Asterisks indicate significant differences from the wild type (*, $P < 0.05$, Student's *t* test).

particular, the strongly disordered PLB lattice in *dgd1* etioplasts suggests that DGDG plays a crucial role in organizing the well-regulated crystalline structure of PLBs. Besides DGDG content, the contents of LPORs and carotenoids decreased in etiolated *dgd1* seedlings. Previous studies showed that PLB size but not PLB lattice structure is affected by LPOR levels (Sperling et al., 1997; Franck et al., 2000; Frick et al., 2003; Masuda et al., 2003, 2009; Paddock et al., 2010). Therefore, the decreased LPOR content in *dgd1* seedlings is not likely the cause of disordered PLB structures. In barley (*Hordeum vulgare*) and Arabidopsis, strongly altered carotenoid composition in etiolated seedlings changed PLB morphology (La Rocca et al., 2001; Park et al., 2002). However, in etiolated *dgd1* seedlings, the carotenoid composition was not largely changed from that in the wild type (Fig. 5). Therefore, DGDG deficiency, but not the associated changes in LPOR and carotenoid levels, may be a primary cause of disordered PLB structures in etiolated *dgd1* seedlings.

We found that the development of PTs also was strongly impaired in etiolated *dgd1* seedlings (Fig. 2, C and I). Considering that the PT membrane has a higher DGDG-to-MGDG ratio than PLBs (Selstam and Sandelius, 1984), DGDG may be particularly important for PT formation. Dörmann et al. (1995) reported that chloroplasts of light-grown *dgd1* plants developed the lamellar thylakoid membrane with stroma thylakoid and stacked grana regions as did wild-type chloroplasts, although the thylakoid membrane was abnormally bent in the mutant. Because light-harvesting complex II (LHCII) proteins, which were normally accumulated in *dgd1* chloroplasts (Härtel et al., 1997), can form lamellar membranes with MGDG in vitro (Garab et al., 2000), DGDG would be unnecessary for the lamellar thylakoid membrane formation. However, in etioplasts, LHCII is almost absent (Kanervo et al., 2008), so non-bilayer-forming MGDG may not be able to form the lamellar PT membrane without bilayer-forming DGDG in *dgd1* etioplasts. Because *dgd1* etioplasts developed PLBs with sizes comparable to those in the wild type despite a strong decrease in DGDG content, another possibility is that a shortage of lipid constituents may lead to impaired growth of PTs. In fact, we previously reported that MGDG deficiency in *amiR-MGD1* seedlings also diminished PT length without affecting PLB size (Fujii et al., 2017). Total galactolipid content, which decreased by 42% in *dgd1* and 26% in *MGD1*-suppressed *amiR-MGD1* relative to the content in control plants, may have a stronger effect on the size of PTs rather than PLBs in etioplasts.

In etiolated *dgd1* seedlings, the protein levels but not the transcript levels of LPORs decreased (Fig. 3, C and D). In addition, the amount of total carotenoids in *dgd1* seedlings decreased without their composition being strongly affected. Because both LPORs and carotenoids are abundant in PTs in addition to PLBs (Selstam and Sandelius, 1984), the severe loss of PTs in *dgd1* may cause a concomitant decrease in these membrane components, with the size of PLBs remaining unaffected. Alternatively, the disordered PLB structure in *dgd1* may inhibit the stable accumulation of LPOR proteins and carotenoids in the membrane.

DGDG Is Required for the Pchlide Biosynthesis Pathway

The enhanced accumulation of Pchlide intermediates instead of Pchlide in ALA-fed *dgd1* seedlings (Fig. 3, E and F) indicates that DGDG deficiency impairs the metabolism from Proto IX to Pchlide. In particular, Mg-Proto IX accumulated in large amounts in *dgd1* seedlings, as observed previously in a knockdown

mutant (*chlm*) of the *CHLM* gene encoding MgMT (Fujii et al., 2017), which suggests that DGDG deficiency strongly impairs the metabolism of Mg-Proto IX to Mg-Proto IX ME in a reaction catalyzed by MgMT. In addition to accumulating Mg-Proto IX, *dgd1* seedlings accumulated Proto IX and Mg-Proto IX ME. Considering that the *chlm* seedlings also accumulated Proto IX, decreased MgMT activity or consequent Mg-Proto IX accumulation might secondarily decrease the metabolism of Proto IX to Mg-Proto IX by MgCh in *dgd1*, although a direct effect of DGDG deficiency on the MgCh activity cannot be excluded. The accumulation of Mg-Proto IX ME in *dgd1* but not *chlm* seedlings suggests that DGDG deficiency inhibits the conversion of Mg-Proto IX ME to Pchlide by MgCY independent of the decreased MgMT activity. The enzymes involved in Pchlide biosynthesis after Proto IX formation are all bound to plastid membranes (Masuda and Fujita, 2008) and may channel porphyrin intermediates to the next enzymes (Tanaka and Tanaka, 2007; Wang and Grimm, 2015). DGDG deficiency and the consequent increase in the proportion of non-bilayer-forming MGDG may change the physical properties of etioplast membranes (Rocha et al., 2018) and may affect these membrane-associated processes in the Pchlide biosynthesis pathway. Notably, the partial MGDG deficiency in etiolated *amiR-MGD1* seedlings also strongly impaired the porphyrin metabolism catalyzed by MgMT and MgCY (Fujii et al., 2017). Thus, the functionality of MgMT and MgCY may be sensitive to the membrane lipid environment in etioplasts. DGDG deficiency may not have severely affected the pathway from ALA to Proto IX, because the sum of Proto IX, Mg-Proto IX, Mg-Proto IX ME, and Pchlide contents was comparable between the wild-type and *dgd1* seedlings. A similar result was observed in *amiR-MGD1* seedlings (Fujii et al., 2017).

DGDG Is Required for the Formation of the Photoactive Pchlide Complex But Not Its Photoconversion Reaction

The decreased activity of the membrane-associated Pchlide biosynthesis pathway caused a decrease in total Pchlide content in etiolated *dgd1* seedlings (Fig. 3A). Notably, in *dgd1* seedlings, photoactive Pchlide content decreased preferentially (Fig. 3A), which indicates that the formation of the photoactive Pchlide-LPOR-NADPH ternary complex decreased in the mutant. Because total LPOR protein levels are associated with the amount of photoactive Pchlide in etioplasts (Sperling et al., 1998; Franck et al., 2000; Masuda et al., 2003), in the *dgd1* seedlings, decreased LPOR level (Fig. 3C) may have resulted in a decreased formation of the photoactive ternary complex. Another possibility is that DGDG deficiency impairs the formation of photoactive complexes independent of reduced LPOR levels. We previously reported that MGDG deficiency in etiolated *amiR-MGD1* seedlings preferentially decreased the amount of the photoactive complex without affecting LPOR protein levels, which suggests a direct involvement of membrane lipids in the formation of the photoactive Pchlide-LPOR-NADPH ternary complex (Fujii et al., 2017). In fact, regeneration of the photoactive ternary complex after flash treatment was retarded in etiolated *dgd1* seedlings (Fig. 4, B–F) as in *amiR-MGD1* seedlings (Fujii et al., 2017), suggesting that DGDG molecules may have a role in the formation of the photoactive complex. Although the ratio of nonphotoactive to photoactive Pchlide increased in *dgd1* seedlings, the absolute amount of the nonphotoactive form was similar to that in the wild type (Fig. 3A), presumably due to parallel impairments of Pchlide biosynthesis and photoactive complex formation in the mutant.

The similar spectral curves of Pchlide fluorescence between wild-type and *dgd1* seedlings (Fig. 4, A and B) appear inconsistent with the quantitative data showing decreased photoactive Pchlide levels in *dgd1* (Fig. 3A). However, this may have resulted from the low quantitative accuracy of the in situ fluorescence spectra obtained directly from cotyledon samples, because of the possibility that emitted fluorescence was resorbed by another pigment in pigment-concentrated structures such as PLBs.

Once the Pchlide-LPOR-NADPH ternary complex was formed in *dgd1*, the Pchlide in the complex was efficiently converted to Chlide with flash treatment as in the wild type (Fig. 4B). The same result was observed in MGDG-deficient *amiR-MGD1* seedlings (Fujii et al., 2017). Furthermore, a previous in vitro assay revealed that membrane lipids do not play essential roles in the photoconversion of Pchlide to Chlide in photoactive complexes (Gabruk et al., 2017). Therefore, galactolipids are important for the formation of the photoactive complex but are not involved directly in the photoconversion reaction of the complex.

We previously reported that MGDG deficiency inhibited the oligomerization of the ternary complex, as reflected by a blue shift of the fluorescence peak at 653 nm to a slightly shorter wavelength in *amiR-MGD1* etioplasts (Fujii et al., 2017). By contrast, DGDG deficiency did not affect this process, as reflected by the prominent fluorescence from the oligomeric ternary complex at 653 nm in *dgd1* as in the wild type (Fig. 4A). This result is consistent with in vitro data that MGDG but not DGDG enhances the oligomerization of the Pchlide-LPOR complex (Gabruk et al., 2017). Although the development of PLBs is strongly associated with the accumulation of the oligomeric Pchlide-LPOR complexes (Schoefs and Franck, 2003), our data suggest that the oligomerization process of the complex is not involved in the disruption of PLB structures in *dgd1* etioplasts (Fig. 2, D and E).

DGDG Is Required for the Disaggregation of Chlide-LPOR Complexes after Photoconversion

The behavior of Chlide-LPOR complexes after photoconversion differed largely between the etiolated wild-type and *dgd1* seedlings (Fig. 4, C–G). In wild-type seedlings, a fluorescence band emerged at 689 nm

after the flash treatment, which would originate from the oligomeric Chlide-LPOR-NADP$^+$ complex, and shifted to ~678 nm within 20 min. This process, the so-called Shibata shift, involves the rapid conversion of the Chlide-LPOR-NADP$^+$ oligomers into the Chlide-LPOR-NADPH oligomers and their disaggregation into the dimeric complex (Shibata, 1957; Smeller et al., 2003; Solymosi et al., 2007). In the *dgd1* seedlings, the Shibata shift was significantly retarded, suggesting that DGDG plays an important role in this process. Notably, in *dgd1* seedlings, the peak Chlide fluorescence was red shifted during the first 5 min after photoconversion, although that in the wild type was blue shifted (Fig. 4, C and G). Because the fluorescence maximum from the oligomeric Chlide-LPOR-NADPH complex is observed at a longer wavelength (~696 nm) than those from the Chlide-LPOR-NADP$^+$ oligomer (~690 nm) and the Chlide-LPOR-NADPH dimer (~682 nm; Schoefs, 2001), in *dgd1* seedlings, Chlide-LPOR-NADPH oligomers may accumulate transiently because of retarded disaggregation, whereas such intermediates are disaggregated rapidly into dimers in the wild type.

MGDG and DGDG Have Different Roles in Etioplast Biogenesis

Together with the previous results obtained with *amiR-MGD1* lines (Fujii et al., 2017), our data suggest different roles of MGDG and DGDG in membrane-associated processes during etioplast development in the dark. Both MGDG and DGDG are required for membrane-associated reactions of the Pchlide biosynthesis pathway and the formation of photoactive complexes in etioplasts. However, MGDG but not DGDG is important for the oligomerization of the photoactive complexes, whereas DGDG plays a specific role in the dissociation of Chlide-LPOR complexes and the formation of the regular lattice PLB structure. The small difference in polar head groups between MGDG and DGDG, with one and two Gal molecules, respectively, largely changes the physicochemical properties of these two galactolipids, as reflected by their differing abilities to form the lamellar bilayer phase (Shipley et al., 1973). This feature may differentiate the roles of MGDG and DGDG during etioplast development.

However, we should note that etiolated *dgd1* seedlings lost more total galactolipid content than *MGD1*-suppressed *amiR-MGD1* seedlings. Thus, we cannot rule out the possibility that, in *dgd1*, an overall deficiency of lipid components in the lipid matrix leads to disturbances in membrane structures. Mutants lacking only MGDG have not been produced, because DGDG is synthesized from MGDG and severe loss of MGDG abolishes DGDG synthesis as well (Kobayashi et al., 2007). Therefore, whether DGDG can form PLBs and PTs and facilitate several membrane-associated processes without MGDG remains to be studied.

MATERIALS AND METHODS

Plant Materials, Growth Conditions, and Light Treatment

The *dgd1* (Dörmann et al., 1995) mutant was in the Columbia ecotype of Arabidopsis (*Arabidopsis thaliana*). Surface-sterilized seeds were incubated in the dark at 4°C for 3 or 4 d and sown on agar (0.8%, w/v)-solidified Murashige and Skoog medium containing 1% (w/v) Suc. They were then preilluminated for 3 h under room light at room temperature before germination in darkness at 23°C. The seedlings were grown for 4 d and harvested under dim green light unless stated otherwise. A single flash of white light for 0.7 ms was used for the photoconversion of photoactive Pchlide to Chlide as described previously (Fujii et al., 2017).

Lipid Analysis

Total lipid extraction, separation with thin-layer chromatography, visualization of lipids, and lipid quantification were performed as described previously (Kobayashi et al., 2006; Fujii et al., 2014, 2017). Contents of MGDG, DGDG, and a mixture of other glycerolipids were analyzed as described previously (Fujii et al., 2017).

Reverse Transcription Quantitative PCR Analysis

Extraction of total RNA from etiolated seedlings, digestion of genomic DNA, reverse transcription, cDNA amplification, and quantification of transcript abundance were performed as described previously (Fujii et al., 2014). Supplemental Table S1 shows the gene-specific primers used in the cDNA amplification.

Immunoblot Analysis

Extraction, quantification, and separation of total proteins from etiolated seedlings as well as detection and quantification of total LPOR proteins were performed as described previously (Fujii et al., 2017). Total proteins (10 µg) were subjected to SDS-PAGE. A primary antibody used in this study was reported previously to react with total LPOR proteins in Arabidopsis (Masuda et al., 2003). Total protein separated by SDS-PAGE and stained with Coomassie Brilliant Blue served as a loading control.

Determination of Pchlide and Total Carotenoid Content

Extraction of Pchlide and carotenoids in 80% (v/v) acetone and determination of the pigments were performed as described previously (Fujii et al., 2017). In brief, Pchlide content was determined by measuring the fluorescence of the extract at 634 nm under 433-nm excitation with a Pchlide standard of known concentration. Total carotenoid content was determined spectrophotometrically by measuring the absorbance of the extract at 470 nm. The amount of nonphotoactive Pchlide was determined by illuminating intact seedlings with a single flash of light before extraction.

ALA Feeding and HPLC Analysis of Porphyrin Pigments

Porphyrin pigments were extracted in *N*,*N*-dimethylformamide from etiolated seedlings fed 10 mM ALA in the dark for 1.5 h and 24 h and quantified by HPLC as described previously (Fujii et al., 2017).

HPLC Analysis of Carotenoids

Carotenoids were extracted in acetone from frozen etiolated seedlings in liquid nitrogen, and the extract was condensed by nitrogen blowing. HPLC analysis was performed as described previously (Kuwabara et al., 1998), with the timing for switching solvent systems modified as described later. The HPLC system consisted of an AG-12 degasser (Eyela), 305 and 306 pumps (Gilson), an 805 manometric module (Gilson), an 811D dynamic mixer (Gilson), a Rheodyne 7725i injector with a 20-µL sample loop (Millipore Sigma), a reverse-phase C18 column (NovaPak, HR, 60 Å, 6 µm, 3.9 × 300 mm; Waters), and a 151 UV/visible detector (Gilson). Data analysis was performed using Clarity version 3.0.7.662 (DataApex). Pigments in 20 µL of extract were eluted with 1.75% (v/v) methanol, 1.75% (v/v) dichloromethane, 1.75% (v/v) ultrapure

water, and 94.75% (v/v) acetonitrile for the first 8 min and 50% (v/v) acetonitrile and 50% (v/v) ethyl acetate for the next 5 min and detected by A_{447}. The flow rate of the mobile phase was 2 mL min^{-1}. Pigments were identified by comparing retention times as described previously (Kuwabara et al., 1998) and absorption spectra of each fraction by using a V-730 BIO spectrophotometer (JASCO). The concentration of each carotenoid pigment was determined by absorption at the peak wavelength and calculated with an extinction coefficient of 140, because the coefficient of carotenoids in the elution solvents was unknown.

In Situ Fluorescence Spectroscopy

Fluorescence emission spectra were obtained from etiolated cotyledons under 440-nm excitation at 77K in liquid nitrogen and normalized as described previously (Fujii et al., 2017). Slit width was 5 nm for both excitation and emission. Data were obtained every 1-nm (for Fig. 4, A–F) and 0.2-nm (for Fig. 4G) wavelength. For analyses of photoconversion and the Shibata shift, flash treatment and the following dark incubation were performed as described previously (Fujii et al., 2017).

Cotyledon Size Measurement

Etiolated cotyledons stuck on adhesive tape were observed and measured as described previously (Fujii et al., 2017).

Measurement of Fresh and Dry Weights

To measure fresh weight, 200 etiolated seedlings were weighed immediately after collection. Seedlings were then dehydrated at 70°C overnight to measure dry weight.

Transmission Electron Microscopy Analysis

Fixation of etiolated cotyledons, sectioning of the fixed samples, staining of the ultrathin sections with uranyl acetate and lead citrate, and observation of the samples by transmission electron microscopy were performed as described previously (Fujii et al., 2017). Quantitative analysis of etioplast ultrastructure was performed as described previously (Fujii et al., 2017), with some modification. Etioplasts with two or more PLBs (fragmented PLBs) were included for analysis, and those without clear PLBs were eliminated. The fragmented PLBs were omitted from the calculation of the circularity index of PLBs.

Statistical Analysis

Statistical significance ($P < 0.05$) was determined by Welch's t test for the data in Figure 2 and by Student's t test for all other quantitative data.

Accession Numbers

Sequence data of the genes investigated in this article can be found in The Arabidopsis Information Resource under the following accession numbers: DGD1 (AT3G11670) ACT8 (AT1G49240), PORA (AT5G54190), PORB (AT4G27440), and PORC (AT1G03630).

Supplemental Data

The following supplemental materials are available.

Supplemental Figure S1. Absolute amounts of membrane glycerolipids in 4-d-old etiolated seedlings.

Supplemental Figure S2. Ultrastructure of etioplasts in 4-d-old etiolated seedlings.

Supplemental Figure S3. Fresh and dry weights of 4-d-old etiolated seedlings.

Supplemental Table S1. Oligonucleotide primers used for reverse transcription quantitative PCR analysis.

ACKNOWLEDGMENTS

We thank Peter Dörmann (Department of Molecular Biotechnology, Institute of Molecular Physiology and Biotechnology of Plants, University of Bonn) for supplying the *dgd1* mutant and Megumi Kobayashi (Department of Chemical and Biological Sciences, Faculty of Science, Japan Women's University) for technical assistance with transmission electron microscopy analysis.

Received February 21, 2018; accepted June 13, 2018; published June 26, 2018.

LITERATURE CITED

Beale SI (1999) Enzymes of chlorophyll biosynthesis. Photosynth Res **60**: 43–73

Benning C, Ohta H (2005) Three enzyme systems for galactoglycerolipid biosynthesis are coordinately regulated in plants. J Biol Chem **280**: 2397–2400

Brentel I, Selstam E, Lindblom G (1985) Phase equilibria of mixtures of plant galactolipids: the formation of a bicontinuous cubic phase. Biochim Biophys Acta **812**: 816–826

Brzezowski P, Richter AS, Grimm B (2015) Regulation and function of tetrapyrrole biosynthesis in plants and algae. Biochim Biophys Acta **1847**: 968–985

Dörmann P, Hoffmann-Benning S, Balbo I, Benning C (1995) Isolation and characterization of an *Arabidopsis* mutant deficient in the thylakoid lipid digalactosyl diacylglycerol. Plant Cell **7**: 1801–1810

Dorne AJ, Joyard J, Douce R (1990) Do thylakoids really contain phosphatidylcholine? Proc Natl Acad Sci USA **87**: 71–74

Franck F, Beraza B, Böddi B (1999) Protochlorophyllide-NADP+ and protochlorophyllide-NADPH complexes and their regeneration after flash illumination in leaves and etioplast membranes of dark-grown wheat. Photosynth Res **59**: 53–61

Franck F, Sperling U, Frick G, Pochert B, van Cleve B, Apel K, Armstrong GA (2000) Regulation of etioplast pigment-protein complexes, inner membrane architecture, and protochlorophyllide a chemical heterogeneity by light-dependent NADPH:protochlorophyllide oxidoreductases A and B. Plant Physiol **124**: 1678–1696

Frick G, Su Q, Apel K, Armstrong GA (2003) An Arabidopsis porB porC double mutant lacking light-dependent NADPH:protochlorophyllide oxidoreductases B and C is highly chlorophyll-deficient and developmentally arrested. Plant J **35**: 141–153

Fujii S, Kobayashi K, Nakamura Y, Wada H (2014) Inducible knockdown of MONOGALACTOSYLDIACYLGLYCEROL SYNTHASE1 reveals roles of galactolipids in organelle differentiation in Arabidopsis cotyledons. Plant Physiol **166**: 1436–1449

Fujii S, Kobayashi K, Nagata N, Masuda T, Wada H (2017) Monogalactosyldiacylglycerol facilitates synthesis of photoactive protochlorophyllide in etioplasts. Plant Physiol **174**: 2183–2198

Gabruk M, Myśliwa-Kurdziel B, Kruk J (2017) MGDG, PG and SQDG regulate the activity of light-dependent protochlorophyllide oxidoreductase. Biochem J **474**: 1307–1320

Garab G, Lohner K, Laggner P, Farkas T (2000) Self-regulation of the lipid content of membranes by non-bilayer lipids: a hypothesis. Trends Plant Sci **5**: 489–494

Härtel H, Lokstein H, Dörmann P, Grimm B, Benning C (1997) Changes in the composition of the photosynthetic apparatus in the galactolipid-deficient dgd1 mutant of *Arabidopsis thaliana*. Plant Physiol **115**: 1175–1184

Heyes DJ, Hunter CN (2005) Making light work of enzyme catalysis: protochlorophyllide oxidoreductase. Trends Biochem Sci **30**: 642–649

Kanervo E, Singh M, Suorsa M, Paakkarinen V, Aro E, Battchikova N, Aro EM (2008) Expression of protein complexes and individual proteins upon transition of etioplasts to chloroplasts in pea (*Pisum sativum*). Plant Cell Physiol **49**: 396–410

Kelly AA, Froehlich JE, Dörmann P (2003) Disruption of the two digalactosyldiacylglycerol synthase genes DGD1 and DGD2 in *Arabidopsis* reveals the existence of an additional enzyme of galactolipid synthesis. Plant Cell **15**: 2694–2706

Kobayashi K, Masuda T, Takamiya K, Ohta H (2006) Membrane lipid alteration during phosphate starvation is regulated by phosphate signaling and auxin/cytokinin cross-talk. Plant J **47**: 238–248

Kobayashi K, Kondo M, Fukuda H, Nishimura M, Ohta H (2007) Galactolipid synthesis in chloroplast inner envelope is essential for proper thylakoid

biogenesis, photosynthesis, and embryogenesis. Proc Natl Acad Sci USA **104**: 17216–17221

Kobayashi K, Awai K, Nakamura M, Nagatani A, Masuda T, Ohta H (2009a) Type-B monogalactosyldiacylglycerol synthases are involved in phosphate starvation-induced lipid remodeling, and are crucial for low-phosphate adaptation. Plant J **57**: 322–331

Kobayashi K, Nakamura Y, Ohta H (2009b) Type A and type B monogalactosyldiacylglycerol synthases are spatially and functionally separated in the plastids of higher plants. Plant Physiol Biochem **47**: 518–525

Kuwabara T, Hasegawa M, Takaichi S (1998) Reaction system for violaxanthin de-epoxidase with PSII membranes. Plant Cell Physiol **39**: 16–22

La Rocca N, Rascio N, Oster U, Rüdiger W (2001) Amitrole treatment of etiolated barley seedlings leads to deregulation of tetrapyrrole synthesis and to reduced expression of Lhc and RbcS genes. Planta **213**: 101–108

Masuda T (2008) Recent overview of the Mg branch of the tetrapyrrole biosynthesis leading to chlorophylls. Photosynth Res **96**: 121–143

Masuda T, Fujita Y (2008) Regulation and evolution of chlorophyll metabolism. Photochem Photobiol Sci **7**: 1131–1149

Masuda S, Ikeda R, Masuda T, Hashimoto H, Tsuchiya T, Kojima H, Nomata J, Fujita Y, Mimuro M, Ohta H, (2009) Prolamellar bodies formed by cyanobacterial protochlorophyllide oxidoreductase in Arabidopsis. Plant J **58**: 952–960

Masuda T, Fusada N, Oosawa N, Takamatsu K, Yamamoto YY, Ohto M, Nakamura K, Goto K, Shibata D, Shirano Y, (2003) Functional analysis of isoforms of NADPH:protochlorophyllide oxidoreductase (POR), PORB and PORC, in *Arabidopsis thaliana*. Plant Cell Physiol **44**: 963–974

Moellering ER, Muthan B, Benning C (2010) Freezing tolerance in plants requires lipid remodeling at the outer chloroplast membrane. Science **330**: 226–228

Oosawa N, Masuda T, Awai K, Fusada N, Shimada H, Ohta H, Takamiya K (2000) Identification and light-induced expression of a novel gene of NADPH-protochlorophyllide oxidoreductase isoform in *Arabidopsis thaliana*. FEBS Lett **474**: 133–136

Oster U, Rüdiger W (1997) The G4 gene of *Arabidopsis thaliana* encodes a chlorophyll synthase of etiolated plants. Bot Acta **110**: 420–423

Ouazzani Chahdi MA, Schoefs B, Franck F (1998) Isolation and characterization of photoactive complexes of NADPH:protochlorophyllide oxidoreductase from wheat. Planta **206**: 673–680

Paddock TN, Mason ME, Lima DF, Armstrong GA (2010) Arabidopsis protochlorophyllide oxidoreductase A (PORA) restores bulk chlorophyll synthesis and normal development to a porB porC double mutant. Plant Mol Biol **72**: 445–457

Park H, Kreunen SS, Cuttriss AJ, DellaPenna D, Pogson BJ (2002) Identification of the carotenoid isomerase provides insight into carotenoid biosynthesis, prolamellar body formation, and photomorphogenesis. Plant Cell **14**: 321–332

Rocha J, Nitenberg M, Girard-Egrot A, Jouhet J, Maréchal E, Block MA, Breton C (2018) Do galactolipid synthases play a key role in the biogenesis of chloroplast membranes of higher plants? Front Plant Sci **9**: 126

Rowe JD, Griffiths WT (1995) Protochlorophyllide reductase in photosynthetic prokaryotes and its role in chlorophyll synthesis. Biochem J **311**: 417–424

Schaller S, Latowski D, Jemioła-Rzemińska M, Wilhelm C, Strzałka K, Goss R (2010) The main thylakoid membrane lipid monogalactosyldiacylglycerol (MGDG) promotes the de-epoxidation of violaxanthin associated with the light-harvesting complex of photosystem II (LHCII). Biochim Biophys Acta **1797**: 414–424

Schoefs B (2001) The protochlorophyllide-chlorophyllide cycle. Photosynth Res **70**: 257–271

Schoefs B, Bertrand M (2000) The formation of chlorophyll from chlorophyllide in leaves containing proplastids is a four-step process. FEBS Lett **486**: 243–246

Schoefs B, Franck F (2003) Protochlorophyllide reduction: mechanisms and evolutions. Photochem Photobiol **78**: 543–557

Schoefs B, Bertrand M, Funk C (2000) Photoactive protochlorophyllide regeneration in cotyledons and leaves from higher plants. Photochem Photobiol **72**: 660–668

Selstam E, Sandelius AS (1984) A comparison between prolamellar bodies and prothylakoid membranes of etioplasts of dark-grown wheat concerning lipid and polypeptide composition. Plant Physiol **76**: 1036–1040

Shibata K (1957) Spectroscopic studies on chlorophyll formation in intact leaves. J Biochem **44**: 147–173

Shipley GG, Green JP, Nichols BW (1973) The phase behavior of monogalactosyl, digalactosyl, and sulphoquinovosyl diglycerides. Biochim Biophys Acta **311**: 531–544

Smeller L, Solymosi K, Fidy J, Böddi B (2003) Activation parameters of the blue shift (Shibata shift) subsequent to protochlorophyllide phototransformation. Biochim Biophys Acta **1651**: 130–138

Solymosi K, Schoefs B (2010) Etioplast and etio-chloroplast formation under natural conditions: the dark side of chlorophyll biosynthesis in angiosperms. Photosynth Res **105**: 143–166

Solymosi K, Smeller L, Ryberg M, Sundqvist C, Fidy J, Böddi B (2007) Molecular rearrangement in POR macrodomains as a reason for the blue shift of chlorophyllide fluorescence observed after phototransformation. Biochim Biophys Acta **1768**: 1650–1658

Sperling U, van Cleve B, Frick G, Apel K, Armstrong GA (1997) Overexpression of light-dependent PORA or PORB in plants depleted of endogenous POR by far-red light enhances seedling survival in white light and protects against photooxidative damage. Plant J **12**: 649–658

Sperling U, Franck F, van Cleve B, Frick G, Apel K, Armstrong GA (1998) Etioplast differentiation in *Arabidopsis*: both PORA and PORB restore the prolamellar body and photoactive protochlorophyllide-F655 to the cop1 photomorphogenic mutant. Plant Cell **10**: 283–296

Su Q, Frick G, Armstrong G, Apel K (2001) POR C of *Arabidopsis thaliana*: a third light- and NADPH-dependent protochlorophyllide oxidoreductase that is differentially regulated by light. Plant Mol Biol **47**: 805–813

Tanaka R, Tanaka A (2007) Tetrapyrrole biosynthesis in higher plants. Annu Rev Plant Biol **58**: 321–346

Tanaka R, Kobayashi K, Masuda T (2011) Tetrapyrrole metabolism in *Arabidopsis thaliana*. The Arabidopsis Book **9**: e0145, doi/10.1199/tab.0145

Wang P, Grimm B (2015) Organization of chlorophyll biosynthesis and insertion of chlorophyll into the chlorophyll-binding proteins in chloroplasts. Photosynth Res **126**: 189–202

Williams WP, Selstam E, Brain T (1998) X-ray diffraction studies of the structural organisation of prolamellar bodies isolated from Zea mays. FEBS Lett **422**: 252–254